*J. Fluid Mech.* (1989), *vol.* 203, *pp.* 1–22
*Printed in Great Britain*



# Blow-up of unsteady two-dimensional Euler and Navier–Stokes solutions having stagnation-point form

By S. CHILDRESS[1], G. R. IERLEY[2], E. A. SPIEGEL[3] AND W. R. YOUNG[4]

[1] Courant Institute of Mathematical Sciences, New York University, New York, NY 10014, USA

[2] Fluids Research Oriented Group, Department of Mathematical Sciences, Michigan Technological Institute, Houghton, MI 49931, USA

[3] Astronomy Department, Columbia University, New York, NY 10027, USA

[4] Scripps Institution of Oceanography, A-021, University of California at San Diego, La Jolla, CA 92093, USA

(Received 16 February 1988)

The time-dependent form of the classic, two-dimensional stagnation-point solution of the Navier–Stokes equations is considered. If the viscosity is zero, a class of solutions of the initial-value problem can be found in closed form using Lagrangian coordinates. These solutions exhibit singular behaviour in finite time, because of the infinite domain and unbounded initial vorticity. Thus, the blow-up found by Stuart in three dimensions using the stagnation-point form, also occurs in two. The singularity vanishes under a discrete, finite-dimensional 'point vortex' approximation, but is recovered as the number of vortices tends to infinity. We find that a small positive viscosity does not arrest the breakdown, but does strongly alter its form. Similar results are summarized for certain Boussinesq stratified flows.

## 1. Introduction

The question of finite-time blow-up of Euler and Navier–Stokes flows in three dimensions is an interesting theoretical problem with important physical implications. Stuart (1987) has summarized the recent history of the problem, and given new examples of blow-up in finite time of solutions of Euler's equations in an unbounded domain. His solutions have a velocity field of the form $(u, v, w) = (f(x, t), yg(x, t), zh(x, t))$, which is a special case of what shall be referred to here as *stagnation-point similitude*. For Euler's equations, Stuart's approach emphasizes the value of Lagrangian variables in the analysis of singularities. Since the above form (as well as its generalization, see §5) allows an analogous substitution in the viscous Navier–Stokes equations, there is a related class of Navier–Stokes solutions. The examples given by Stuart were suggested by the rapidly growing vortex structures seen in fully developed shear flows. Because of the importance of this singular structure to an understanding of breakdown at transition, it is of interest to assess what, if any, role the stagnation-point similitude might play in its creation.

The two-dimensional Euler and Navier–Stokes equations provide such an opportunity because it is known that, in a bounded domain, a flow, if smooth initially, remains smooth for all time (see below). If a two-dimensional stagnation-

point flow develops singularities then these must be a consequence of the unbounded domain and therefore unphysical; in that case three-dimensional results based on stagnation-point similitude are vulnerable to an analogous criticism.

Like Stuart, we shall concentrate in this paper on stagnation-point flow possessing local similitude. A steady example arises when a stream function of the form $yf(x)$ is introduced, which leads to an ordinary differential equation for $f(x)$. A familiar example is the flow studied by Hiemenz, and later by Howarth (1951) (see Batchelor 1967, p. 28). Here $f(0) = f_x(0) = 0$ and $f_x = -1$ at $x = \infty$. This corresponds to a stagnation-point outer flow with stream function $-xy$, hence to a flow from positive $x$ which impinges on a solid wall at $x = 0$. The boundary layer extends to $|y| = \infty$ in $x \geqslant 0$, with characteristic thickness independent of $x$.

Our purpose here is to investigate a class of unsteady, two-dimensional problems with linear dependence in one or more dependent variables, the substitution $(u, v) = (\psi_y, -\psi_x) = (f(x,t), -yf_x(x,t))$ being our principal example. Substitution into the vorticity equation

$$\omega_t + u\omega_x + v\omega_y - \nu\nabla^2\omega = 0, \quad \omega = -\nabla^2\psi \tag{1.1}$$

yields, after one integration, the following partial differential equation for $f(x,t)$:

$$f_{xt} + ff_{xx} - f_x^2 - \nu f_{xxx} = h(t), \tag{1.2a}$$

where $h(t)$ is an arbitrary function. We shall be interested in the initial-value problem for $f$ in the interval $0 \leqslant x \leqslant L$ subject to the conditions of no slip at the boundary points $x = 0, L$:

$$f(0,t) = f(L,t) = 0, \tag{1.2b}$$

$$f_x(0,t) = f_x(L,t) = 0 \quad \text{for} \quad t > 0. \tag{1.2c}$$

Given (1.2) we may then integrate from 0 to $L$ to obtain an equation for $h(t)$:

$$h(t) = -L^{-1}\left[2\int_0^L f_x^2\,\mathrm{d}x + \nu f_{xx}(L) - \nu f_{xx}(0)\right]. \tag{1.3}$$

If the kinematic viscosity, $\nu$, is zero, then (1.2$a$) reduces to the analogous Euler problem,

$$f_{xt} + ff_{xx} - f_x^2 = h(t), \tag{1.4}$$

and the last two conditions in (1.2$c$) must be dropped. The resulting problem is considered in the next section, where we shall show that a smooth, bounded solution becomes singular after a finite time. Hölder (1933), Wolibner (1933), and more recently Kato (1967) have proved that this cannot happen for bounded initial values and a bounded domain, so this breakdown is a consequence of the linear dependence in $y$ in the strip $0 \leqslant x \leqslant L$. Nevertheless, vorticity is an integral part of the structure of these singular solutions and they provide a simple and useful testing ground for various ideas and methods which are applicable also to the much harder initial-value problem in three dimensions.

For example, in §3 we examine an approximate, discrete representation of the solution of the Euler problem, analogous to a 'vortex method' for two-dimensional inviscid incompressible flow. In this approximation $f$ is a piecewise linear function of $x$. The points of discontinuity, which we shall refer to as 'kinks', are points where the vorticity is concentrated. (Actually each such point determines a vortex sheet parallel to the $y$-axis, the strength of which is proportional to $y$.) Numerical solutions of the discrete system show that $f$ remains bounded for all time, but that the maximum amplitude tends to infinity as the number of kinks increases. Moreover, we

recover the breakdown time as the limit of these times of maximum amplitude. This calculation provides a useful example of how a finite-dimensional representation approximates the singularities of an infinite-dimensional system.

It might be thought that global existence would hold for solutions of the Navier–Stokes problem (1.2), (1.3), but this is apparently not the case, as we shall show in §4. There we prove that for sufficiently small initial Reynolds numbers the flow decays to zero, but find numerically that sufficiently large initial Reynolds numbers produce finite-time blow-up. Moreover, the viscous singularities appear to have a richer structure than conventional boundary-layer theory would suggest.

In the final section we summarize our results and discuss various aspects of the question of singularities of flows in two or three dimensions, emphasizing the special nature of the stagnation-point solutions. We also indicate another class of problems, involving a stratified, Boussinesq fluid in a gravitational field, which can be solved by these methods. An example is worked out in detail in Appendix B.

## 2. Inviscid solutions

We define the operator L on a function, $q(x,t)$, by

$$\mathrm{L}[q] = q_t + fq_x - qf_x. \tag{2.1}$$

We also introduce the Lagrangian coordinate $x(x_0,t)$ satisfying

$$x_t = f(x,t) \tag{2.2a}$$

and

$$x(x_0,0) = x_0. \tag{2.2b}$$

We denote differentiation of $q$ with respect to $t$ with $x_0$ fixed by $\dot{q}$ and thus $\dot{q} = q_t + fq_x$. The Jacobian $J$ of the transformation to Lagrangian variables is defined by $J \equiv \partial x/\partial x_0$ and is initially unity. Differentiating (2.2$a$) with respect to $x_0$ we find

$$\dot{J} = f_x J, \tag{2.3}$$

i.e. $\mathrm{L}[J] = 0$. An equation of the form $\mathrm{L}[q] = R(x_0,t)$ can therefore be solved by variation of parameters by setting $q = JQ$ and noting that $\dot{q} = \dot{J}Q + J\dot{Q} = f_x q + J\dot{Q}$ and therefore $\dot{Q} = J^{-1}R$. For convenience we introduce $\phi = 1/J$. In particular, because $\mathrm{L}[J] = 0$, we see that $f_x = \phi\dot{J} = -\dot{\phi}/\phi$.

We are now prepared to solve (1.2) with $\nu = 0$ under the conditions

$$f(x,0) = f_0(x_0), \quad f(0,t) = f(L,t) = 0, \tag{2.4}$$

where $f_0''(x_0)$ is assumed to be continuous for $0 < x < L$. We consider three different methods for solving the problem for general $f_0$. The first two are related and rely on a transformation to Lagrangian variables, the second method being the two-dimensional version of the Lagrangian method used by Stuart (1987). The third method, while less general than the first two, uses Eulerian variables and is more direct in some cases.

### 2.1. *The first method*

Because $f_x = -\dot{\phi}J$ from (2.3), substitution into (1.2$a$) yields (by the procedure just given) the following problem for $\phi(x_0,t)$:

$$\ddot{\phi} + h(t)\,\phi = 0, \quad \phi(x_0,0) = 1, \quad \dot{\phi}(x_0,t) = \phi_0(x_0), \tag{2.5}$$

where $\phi_0 = -f_0'(x_0)$. We write the solution of (2.5) in the form

$$\phi(x_0, t) = \phi_1(t) + \phi_0(x_0)\,\phi_2(t) \tag{2.6a}$$

in terms of linearly independent solutions $\phi_1$ and $\phi_2$, with

$$\boldsymbol{\Phi}(t) = \begin{bmatrix} \phi_1 & \phi_2 \\ \dot{\phi}_1 & \dot{\phi}_2 \end{bmatrix}, \quad \boldsymbol{\Phi}(0) = \begin{bmatrix} 1 & 0 \\ 0 & 1 \end{bmatrix}. \tag{2.6b}$$

The function $h(t)$ will be determined by (1.2$b$), because the vanishing of $f$ at the endpoints implies that $x(0,t) = 0$ and $x(L,t) = L$. Integrating $J$ we thus have

$$L = \int_0^L \phi^{-1}\,\mathrm{d}x_0 = \int_0^L [\phi_1(t) + \phi_0(x_0)\,\phi_2(t)]^{-1}\,\mathrm{d}x_0. \tag{2.7}$$

This yields a relation of the form $F(\phi_1, \phi_2) =$ constant. Since Lagrangian coordinates must be one–one we assume that the integrand in the last expression is well behaved. Differentiating with respect to $t$, we obtain (with subscripts denoting partials)

$$F_{11}\dot{\phi}_1^2 + 2F_{12}\dot{\phi}_1\dot{\phi}_2 + F_{22}\dot{\phi}_2^2 + F_1\ddot{\phi}_1 + F_2\ddot{\phi}_2 = 0. \tag{2.8}$$

This yields

$$h(t) = \frac{F_{11}\dot{\phi}_1^2 + 2F_{12}\dot{\phi}_1\dot{\phi}_2 + F_{22}\dot{\phi}_2^2}{F_1\phi_1 + F_2\phi_2}. \tag{2.9}$$

If, for example, $\phi_1$ can be obtained as an explicit function of $\phi_2$, $G(\phi_2)$ say, then a second-order nonlinear equation for $\phi_2$ can be obtained. In general, an equation of the form

$$\dot{\boldsymbol{\Phi}} = \boldsymbol{P}(\boldsymbol{\Phi}) \tag{2.10}$$

results, where $\boldsymbol{P}$ is a certain nonlinear matrix function of the elements of the fundamental solution matrix $\boldsymbol{\Phi}$, as determined by (2.9).

### 2.2. *An example*

Suppose that

$$f_0 = \tfrac{1}{2}x_0(2 - x_0), \quad L = 2, \quad \phi_0 = x_0 - 1. \tag{2.11}$$

From (2.7) we then obtain

$$\phi_1 = G(\phi_2) = \phi_2 \coth(\phi_2). \tag{2.12}$$

Thus

$$h = \frac{G''\dot{\phi}_2^2}{\phi_2 G' - G} \tag{2.13}$$

is used in the equation for $\phi_2$; the result is easily integrated once and we have

$$\dot{\phi}_2 = [\sinh(\phi_2)/\phi_2]^2. \tag{2.14}$$

From (2.6) and (2.12) there results

$$J = [\sinh(\phi_2)/\phi_2][\cosh(\phi_2) + (x_0 - 1)\sinh(\phi_2)]^{-1}. \tag{2.15}$$

We may now obtain $x(x_0, t)$ by integration of (2.15) with respect to $x_0$. Letting $\tau = \phi_2$ we obtain

$$x = \tau^{-1}\ln(1 + x_0\,\mathrm{e}^{\tau}\sinh\tau). \tag{2.16}$$

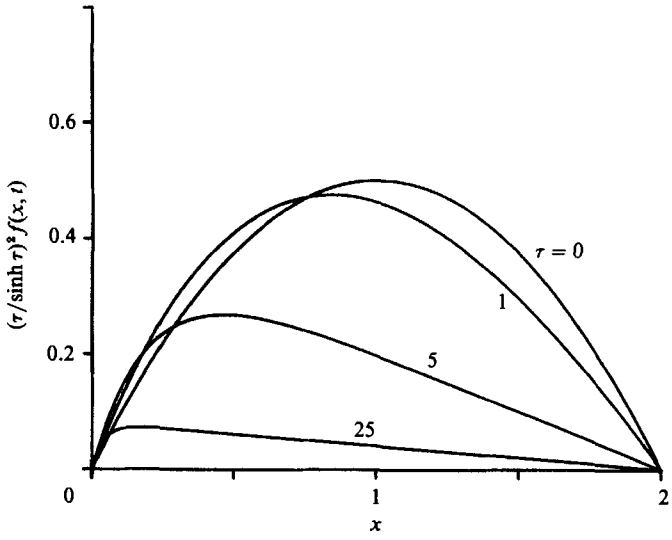


FIGURE 1. $(\tau/\sinh\tau)^2 f(x,t)$ at $\tau = 0$, 1, 5 and 25. At this last instant, $(\sinh\tau/\tau)^2 = 2.1\times10^{18}$ and $t = t^* - 2.51\times10^{-19}$.

Finally, we may find $f(x,t)$ by differentiating (2.16) with respect to $t$ and eliminating $x_0$ in favour of $x$:

$$f(x,t) = \left[\frac{2(e^{2\tau}-e^{(2-x)\tau})}{\tau(e^{2\tau}-1)} - \frac{x}{\tau}\right]\left(\frac{\sinh\tau}{\tau}\right)^2. \tag{2.17}$$

Noting that

$$t(\tau) = \int_0^\tau \sigma^2/\sinh^2(\sigma)\,d\sigma, \quad t(\infty) = \int_0^1 \frac{\ln s}{s-1}ds = \tfrac{1}{6}\pi^2 = t^*, \tag{2.18}$$

we observe that $f$ as given by (2.17) becomes unbounded at time $t^*$, with

$$\tau(t) \sim -\tfrac{1}{2}\ln(t^*-t) + \ln\left(\frac{|\ln(t^*-t)|}{\sqrt{2}}\right) + o(1) \tag{2.19}$$

as breakdown is approached. We show $f(x,t)$ in figure 1. Near $t^*$ we see that, away from endpoints, $f$ grows like $(2-x)\dot{\tau}/\tau$. Thus the velocity grows while the flow becomes irrotational over the interior (since $f_{xx} \approx 0$ there and vorticity $= -yf_{xx}$).

This growth is supported by the increase of vorticity near $x = 0$. It is helpful to think of a given layer $y =$ constant in a channel of width 2. Because the initial vorticity increases indefinitely with $y$, the downflow occurring initially in the region $0 < x < 1$, and thereafter near $x = 0$, has the effect of bringing down large vorticity from high in the channel. Indeed we observe that $v = \dot{y} = -yf_x = -y\dot{J}/J$ or $y(x_0, y_0, t) = y_0/J$. Thus, $y(0, y_0, t) = y_0/(\dot{\tau}\,e^{\tau})$ and so arbitrarily large vorticity is advected to the layer in question within time $t^*$. We thus conclude that the singularity forms as a result of the unboundedness of initial vorticity. On the other hand the singularity is a consequence of Euler's equations within this class of solutions; no arbitrary functions or parameters have been *manipulated to* produce it.

### 2.3. *The second method*

We now describe an alternative method for producing a general solution to $\mathrm{L}[f_{xx}] = 0$. It is less direct than the first method, but parallels closely the general formal solution of Euler's equations in Lagrangian coordinates. Since $\mathrm{L}[J] = 0$ our equation can clearly be solved exactly in the form

$$f_{xx} = f_0''(x_0)\, J(x_0, t). \tag{2.20}$$

This is the present version of Cauchy's integration of the vorticity equation using Lagrangian coordinates (Batchelor 1967, p. 276). To obtain the corresponding Biot–Savart integral, expressing velocity in terms of vorticity, we may simply multiply (2.20) by $J$ and integrate with respect to $x_0$. If we define $s \equiv 2f_0'$ we see that

$$2f_x = \int J^2 \,\mathrm{d}s. \tag{2.21}$$

Note that the initial condition can be absorbed into a single independent variable $s$. If we set $f_x = \dot{J}/J = \frac{1}{2}\dot{H}$, then we obtain after a differentiation of (2.21) with respect to $s$

$$H_{st} = \mathrm{e}^H, \quad H(s,0) = 0. \tag{2.22}$$

This is Liouville's equation, the general solution of which can be found in closed form (see e.g. Drazin 1983, chap. 7). Note, however, that we have reduced the problem of solving $\mathrm{L}[f_{xx}] = 0$ to the finding of a *particular* solution of (2.22). Also to ensure that the transformation from $x_0$ to $x$ is one–one, we shall require that $f_0'' \neq 0$ in the interval $0 < x_0 < L$, a condition that is not needed using the first method.

For our purposes it is sufficient to note that an exact solution of $\mathrm{L}[f_{xx}] = 0$ is $f = A\sin(Bx)$, where $A$ and $B$ are arbitrary constants. For this steady solution we may evaluate the Jacobian by solving (2.2). The result is

$$J = [\cosh(kt) - (s/2k)\sinh(kt)]^{-1}, \quad k = AB. \tag{2.23}$$

In order to satisfy the boundary conditions on $f$ we need an arbitrary function of time, not present in (2.23). However, we have the following easily proved result: if $\tilde{H}(s,t)$ is a solution of (2.22), so is $H(s,\tau) = \ln(\dot{\tau}(t)) + \tilde{H}(s,\tau)$, where $\tau$ is any function of $t$ satisfying $\dot{\tau}(0) = 1, \tau(0) = 0, \dot{\tau}(t) > 0$. Thus we obtain the general solution of (2.22) in the form

$$J = \frac{\dot{\tau}^{\frac{1}{2}}}{\cosh k\tau - (s/2k)\sinh k\tau}. \tag{2.24}$$

Here $k$ is an arbitrary constant which can be chosen, given $f_0$, so that the denominator in (2.24) does not vanish. At this point (2.24) stands as a general solution, even for an $f_0$ whose second derivative vanishes somewhere in the interior.

The equation which determines $\tau(t)$ is again that $J$ have integral $L$ over the interval:

$$\dot{\tau}^{\frac{1}{2}} \int_0^L \frac{\mathrm{d}x_0}{\cosh k\tau - (s(x_0)/2k)\sinh k\tau} = L. \tag{2.25}$$

For suitably small $k$, this yields a differential equation for $\tau$. Once it is solved, (2.24) may be integrated to obtain $f_x$ and then $f(x,t)$. For the example given above, the equation for $k\tau$ is the same as equation (2.14) for $\phi_2$. The integrations then yield (2.16). We may here take $k = 1$ and require $\max|s(x_0)| \leqslant 1$ although (2.16) is independent of the choice of $k$ as long as (2.25) is defined.

### 2.4. *Solutions on an infinite interval: inviscid stagnation-point and inertial-layer solutions*

It is of interest to make contact with the classical stagnation-point flow (see Batchelor 1967, p. 285) in the unsteady context, although this is a different initial-value problem. We take $L = \infty$ and require that $f_x \to -1$ as $x \to \infty$. Assuming that $-1 \leqslant f_0' \leqslant 0$ we have

$$J = \tau^{\frac{1}{2}}(\cosh\tau - f_0' \sinh\tau)^{-1}. \tag{2.26}$$

Since, for the Lagrangian form of stagnation-point flow, $J \approx \mathrm{e}^{-t}$ for large $x_0$, we see from the above that $\tau = t$. From $f_x = \dot{J}/J$ we then obtain

$$f_x = -\frac{\sinh t - f_0' \cosh t}{\cosh t - f_0' \sinh t}. \tag{2.27}$$

In this solution there is no finite-time singularity since the fluid is inviscid, and vorticity is advected steadily into an ever-smaller layer at the wall. The flow becomes irrotational ($f_x \approx -1$) in infinite time at all positive $x$.

Finite-time singularities are by no means ruled out on an infinite interval, however, even in two dimensions. The solution

$$f = \frac{1 - \mathrm{e}^{-x}}{t^* - t} \tag{2.28}$$

of (1.4) with $h(t) = 0$ is a simple example of a blow-up which occurs even though the vorticity decays exponentially as $x \to \infty$. It represents a time-dependent inertial layer in the domain $x > 0$. A somewhat more complicated inertial-layer solution can be obtained using the method of §2.1, with $h(t) = 0$ in (2.5) and taking $f_0' = \mathrm{e}^{-x_0}(1 - \mathrm{e}^{-x_0})$. Then $\phi = 1 - f_0' t$ and $x$ can be found by integration:

$$x = \tfrac{1}{2}\ln(E^2 - tE + t) + \frac{t}{\Delta}\left[\tan^{-1}\left(\frac{2E - t}{\Delta}\right) - \tan^{-1}\left(\frac{2 - t}{\Delta}\right)\right], \tag{2.29a}$$

where

$$E = \mathrm{e}^{x_0}, \quad \Delta = (4t - t^2)^{\frac{1}{2}}. \tag{2.29b}$$

That a singularity occurs as $t \to 4$ is evident from the local representation of $x(E, t)$ valid for $E - 2$ small and of order $(4 - t)^{\frac{1}{2}}$:

$$x \approx \frac{1}{(4 - t)^{\frac{1}{2}}}\left[\pi + 2\tan^{-1}\left(\frac{E - 2}{(4 - t)^{\frac{1}{2}}}\right)\right]. \tag{2.30}$$

### 2.5. *The third method*

Certain interesting solutions of (1.4) can best be found by direct approach in Eulerian variables. An example is a one-parameter family of separable solutions of the form

$$f(x, t) = \frac{F(x)}{t^* - t} \quad \text{with} \quad N_0 = \int_0^L f_x^2(x, 0)\,\mathrm{d}x. \tag{2.31a, b}$$

Substituting into (1.4) and (1.2$b$) we obtain

$$F' + FF'' - F''^2 = (t^* - t)^2 h(t) \equiv q^2, \quad F(0) = F(L) = 0. \tag{2.32a, b}$$

Of course $q^2$ must be constant and (2.32) implies

$$\int_0^L F'^2\,\mathrm{d}x = \tfrac{1}{2}q^2 L \tag{2.33}$$

and so the blow-up time is

$$t^*(q) = q\left(\frac{L}{2N_0}\right)^{\frac{1}{2}}. \tag{2.34}$$

The problem in (2.33) is now reduced to quadratures by introducing

$$G \equiv F', \tag{2.35a}$$

and writing

$$\begin{aligned} G' &= (G^2 - G - q^2)/F, \\ &= (G-p)(G+p^{-1}q^2)/F, \end{aligned} \tag{2.35b}$$

where

$$p \equiv \tfrac{1}{2}[1+(1+4q^2)^{\frac{1}{2}}]. \tag{2.36}$$

To avoid singularities where $F = 0$, one requires that $G = p$ or $-q^2/p$ at these points. Specifically we suppose $G = -q^2/p$ at $x = 0$. Dividing (2.35$a$) by (2.35$b$) gives a separable equation which can be integrated to yield

$$F = C(p-G)^{\alpha}(G+q^2/p)^{1-\alpha}, \quad \alpha \equiv \frac{p^2}{p^2+q^2}. \tag{2.37a,b}$$

The constant of integration, $C$, is found by requiring that at $x = 0$ and $x = \frac{1}{2}L$, $F = 0$ and $G = -q^2/p$ and $p$ respectively. $F$ is antisymmetric about $x = \frac{1}{2}L$ so that it also vanishes at $x = L$. In fact, one can regard the family of solutions as periodic in $x$ with period $L$. On combining (2.35$b$) and (2.37$a$) one then has

$$x = -C\int_{-q^2/p}^{G} \mathrm{d}G_1 (p-G_1)^{\alpha-1}(G_1+q^2/p)^{-\alpha} \tag{2.38}$$

so that at $x = \frac{1}{2}L$, where $G = p$,

$$\tfrac{1}{2}L = -C\int_{-q^2/p}^{p} \mathrm{d}G_1 (p-G_1)^{\alpha-1}(G_1+q^2/p)^{-\alpha} \tag{2.39a}$$

$$= -C\int_0^1 \mathrm{d}z (1-z)^{\alpha-1} z^{-\alpha} \tag{2.39b}$$

$$= -\pi C/\sin\pi\alpha, \tag{2.39c}$$

or

$$C = -L\sin(\pi\alpha)/2\pi.$$

A simple limiting case is $q^2 \to \infty$ so that $\alpha \to \frac{1}{2}, t^* \to \infty$, and (2.37) is

$$\left(\frac{L}{2\pi}\right)^2 G^2 + F^2 = \left(\frac{qL}{2\pi}\right)^2, \tag{2.40a}$$

or

$$F = -\left(\frac{qL}{2\pi}\right)\sin\left(\frac{2\pi x}{L}\right). \tag{2.40b}$$

It is easy to show by direct substitution that (2.40$b$) is a steady solution of (1.4) (and hence $t^* = \infty$) of (1.4).

The complementary case is $q^2 \to 0$ so that $\alpha \to 1$ and $t^* \to 0$. In this instance $F' \approx -q$ on the entire interval $0 < x < L$ except for an internal boundary layer at $x = \frac{1}{2}L$, of width $q$. This 'sawtooth', which instantly blows up, is essentially identical to a periodic extension of the last profile ($\tau = 25$) in figure 1. As a representative of the family between these limiting extremes for $q$, we plot in figure 2 the case $q = 1$ on the interval $x = 0$ to $x = L = 2$.

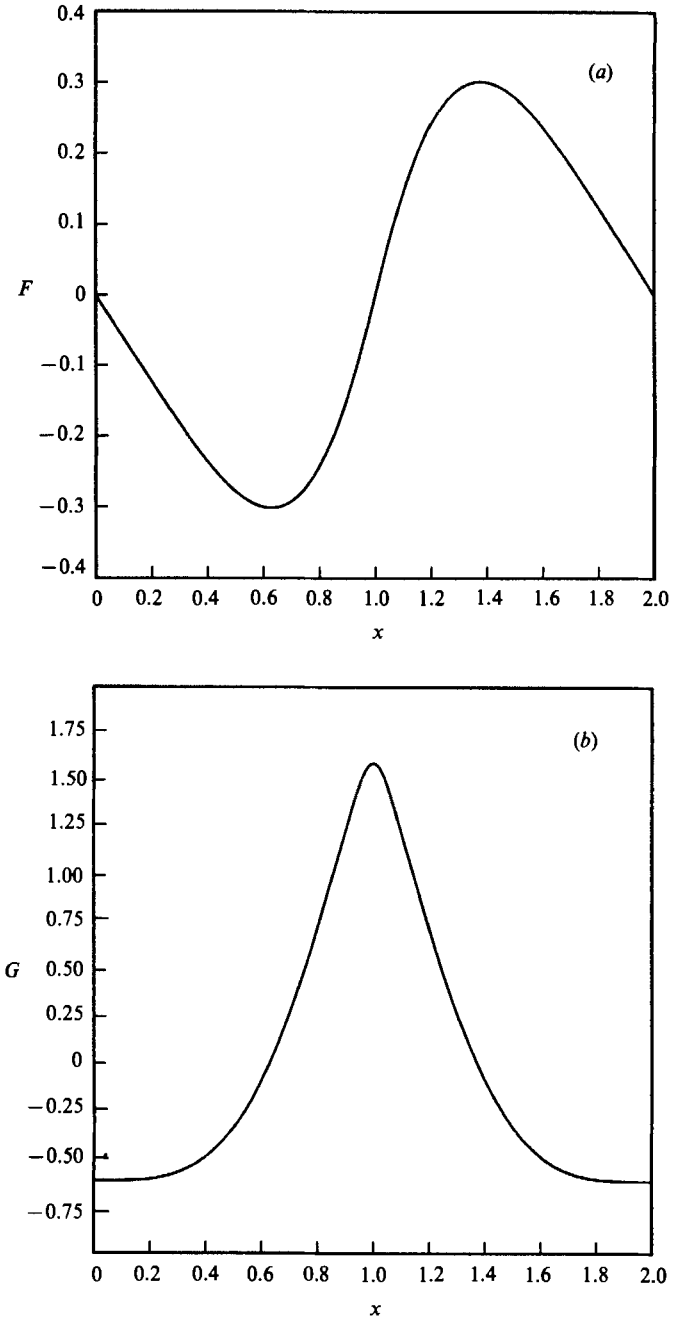


FIGURE 2. The spatial structure of the separable, inviscid solution: (*a*) $F(x)$, (*b*) $G = \mathrm{d}F/\mathrm{d}x$. The normalization is $\int_0^2 G^2\,\mathrm{d}x = 1$.

This one-parameter family of solutions shows that boundary-layer formation, as in (2.17) and illustrated in figure 1, is not essential to finite-time blow-up. This important point will emerge again in §4 where we find that small viscosity does not prevent finite-time blow-up, but it does prevent the concentration of vorticity into increasingly thin boundary layers.

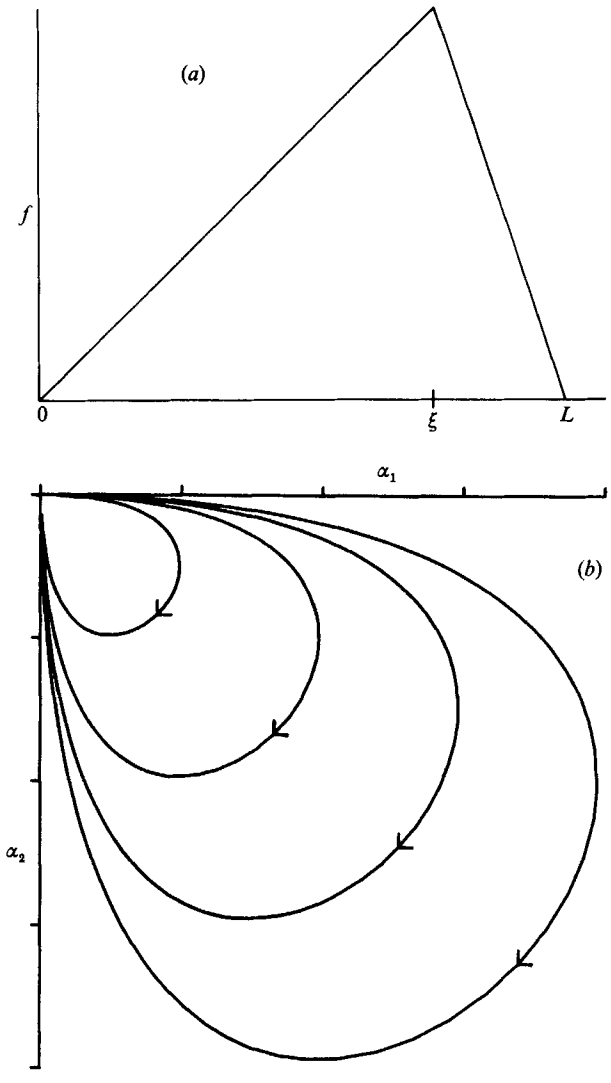


FIGURE 3. (*a*) Definition sketch for the one-kink model. The kink is at $x = \xi$ and the slopes of the two straight-line segments are $\alpha_1$ and $\alpha_2$ as in (3.1 *a*). (*b*) Phase-plane evolution of the system in (3.3). Because $\alpha_1$ and $\alpha_2$ have opposite signs, and $f_{\max} = \alpha_1\alpha_2/(\alpha_1 - \alpha_2)$, there is no singularity and in fact $f_{\max}$ ultimately approaches zero.

## 3. Concentrated vorticity

The aim of the present section is to indicate how point-vortex methods (see e.g. Aref 1983) used in the numerical solution of Euler's equations in two dimensions have a natural counterpart for our inviscid model (1.4). Since irrotational flow corresponds to $f_{xx} = 0$, a flow with concentrated vorticity should be generated by $f$ values that are piecewise linear in $x$. We shall refer to a point where the slope of $f$ is discontinuous as a 'kink'. We shall show that the motion and evolution of kinks provides a natural numerical approximation. Our work will be formal although the relative simplicity of the construction invites a more rigorous approach.

### 3.1. *A one-kink model*

Consider, for example, the single-kink representation shown in figure 3(*a*). We set

$$f = \alpha_1 x, \quad 0 \leqslant x < \xi(t), \quad \text{and} \quad f = \alpha_2(x-L), \quad \xi < x \leqslant L, \tag{3.1a,b}$$

where

$$\alpha_1 \xi = \alpha_2(\xi - L), \tag{3.2a}$$

and then substitution into (1.4) produces two equations for the $\alpha$ together with an equation for the motion of the kink (obtained as a coefficient of a delta function):

$$\dot{\alpha}_1 - \alpha_1^2 = \dot{\alpha}_2 - \alpha_2^2 = h(t), \quad \dot{\xi} = f(\xi, t) = \alpha_1 \xi. \tag{3.2b,c}$$

From (3.2*a*) we obtain $\xi = L\alpha_2/(\alpha_2 - \alpha_1)$, and differentiation using (3.2*b*) produces a second expression for $\dot{\xi}$. Combining this with (3.2*c*) we obtain $h = 2\alpha_1\alpha_2$. This expression for $h$ is consistent with the inviscid form of (1.3) under the substitution (3.1*a*). We thus obtain from (3.2*b*) the autonomous system

$$\dot{\alpha}_1 = \alpha_1^2 + 2\alpha_1\alpha_2, \quad \dot{\alpha}_2 = \alpha_2^2 + 2\alpha_1\alpha_2. \tag{3.3}$$

We sketch the phase plane of this system in figure 3(*b*). The system always evolves towards zero, passing through a maximum amplitude before it decays. There is no finite-time singularity.

### 3.2. *An N-kink model*

For $N > 1$ kinks the situation is similar. Let the kinks be located at points $\xi_i$ in the interval $(0, L)$, with the corresponding slopes $\alpha_1, \ldots, \alpha_{N+1}$ and denote the value of $f$ at $\xi_i$ by $f_i$. With $\xi_0 = f_0 = f_{N+1} = 0, \xi_{N+1} = L$, set

$$f(x) = \alpha_i(x - \xi_i) + f_i, \quad \xi_{i-1} < x < \xi_i, \quad i = 1, \ldots, N+1. \tag{3.4}$$

We then have the following system of equations for $i = 1, \ldots, N$:

$$\dot{\alpha}_i - \alpha_i^2 = h(t), \quad h(t) = -2\sum_{i=1}^{N+1} \alpha_i^2(\xi_i - \xi_{i-1}), \quad \dot{\xi}_i = f_i. \tag{3.5a–c}$$

In addition (3.5*a*) holds for $i = N+1$. Thus (3.5) yields $2(N+1)$ equations for $h, \xi_1, \ldots, \xi_N, \alpha_1, \ldots, \alpha_{N+1}, f_1, \ldots, f_N$. The remaining $N$ equations are the continuity constraints

$$f_i = \alpha_i(\xi_{i+1} - \xi_i), \quad i = 1, \ldots, N. \tag{3.5d}$$

### 3.3. *Calculation of the sample problem*

For the initial function $f_0 = \frac{1}{2}x_0(2 - x_0)$ we solved the system (3.5) for $N = 50, 60, \ldots, 250$. For all $N$ the function $f$ remains finite but the maximum valuc $f_{\max}$ obtained increases with $N$, and this value occurs at a time $t_{\max}$ which approaches $t^*$ as $N$ increases. We show these results in figure 4.

## 4. Viscous effects

We now turn to the behaviour of solutions of (1.2) when $\nu > 0$. We shall show that sufficiently small initial values of $f$ lead to global decay to zero. On the other hand we find, using numerical methods, that the blow-up observed in the inviscid case is not arrested by viscous stresses. This leads us to the conclusion that sufficiently *large* initial conditions continue to produce finite-time blow-up.

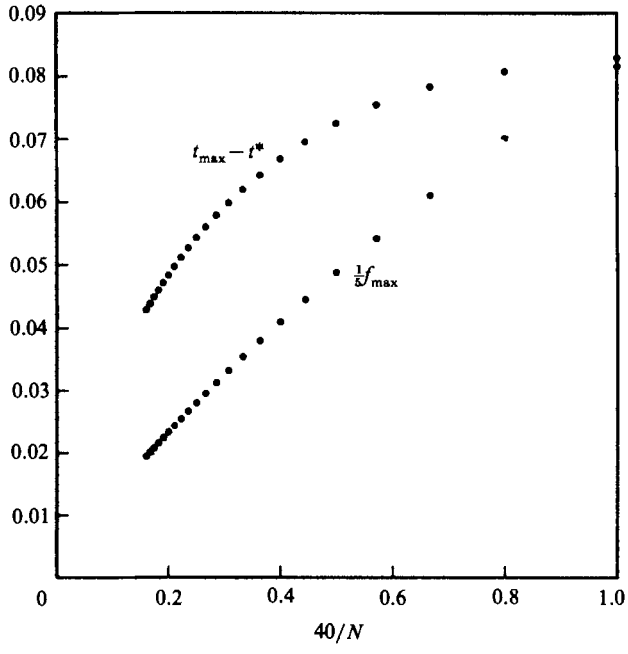


FIGURE 4. How increasing the resolution by using more kinks in the representation (3.4) changes both $f_{max}$ and $t_{max}$. The lowest resolution is $N = 50$ or $40/N = 0.8$, and $N$ was increased in steps of 10 until $N = 250$ or $40/N = 0.16$. There is never any singularity but $f_{max}$ increases as more kinks are used and $t_{max}$ approaches $\pi^2/6$.

### 4.1. *Decay of low-Reynolds-number initial conditions*

To study the question of decay of small solutions, multiply (1.2$a$) by $f_x$ and integrate from 0 to $L$. This leads to an energy integral of the form

$$\dot{N} = 3S - 2\nu D, \tag{4.1a}$$

where
$$N(t) = \int_0^L f_x^2 \,\mathrm{d}x, \quad S(t) = \int_0^L f_x^3 \,\mathrm{d}x, \quad D(t) = \int_0^L f_{xx}^2 \,\mathrm{d}x. \tag{4.1b–d}$$

We now establish the following result: let an initial Reynolds number be defined by

$$R_0 \equiv N_0^{\frac{1}{2}} L^{\frac{3}{2}}/\nu, \tag{4.2}$$

where $N_0 = N(0)$ and similarly for the other variables. Then if $R_0 < 16.212$, $f$ will decay to zero with time. The essential idea is that the function $g \equiv f_x$ has two properties

$$g(0) = g(L) = 0, \quad \int_0^L g \,\mathrm{d}x = 0 \tag{4.3a,b}$$

and all such functions satisfy the inequalities

$$\int_0^L g'^2 \,\mathrm{d}x \geqslant \left(\frac{2\pi}{L}\right)^2 \int_0^L g^2 \,\mathrm{d}x, \tag{4.4a}$$

$$\left\{\int_0^L g'^2 \,\mathrm{d}x\right\}^2 \left\{\int_0^L g^2 \,\mathrm{d}x\right\} \geqslant \gamma^2 L^{-3} \left\{\int_0^L g^3 \,\mathrm{d}x\right\}^2. \tag{4.4b}$$

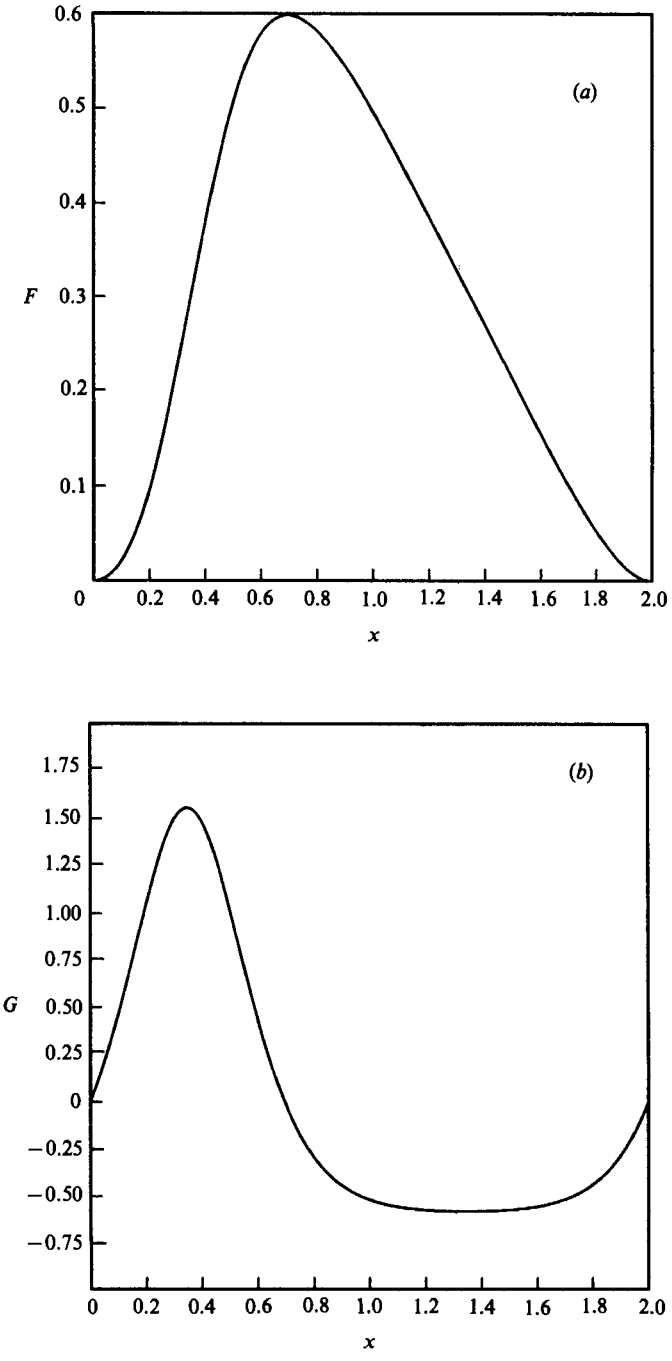


FIGURE 5. The solution of the Euler–Lagrange equation (A 6). (*a*) $f(x)$, (*b*) $g = \mathrm{d}f/\mathrm{d}x$. According to the energy equation (4.1), this initial condition maximizes rate of growth. If $R_0 = N_0^{\frac{1}{2}} L^{\frac{3}{2}}/\nu \leqslant 16.213$ then the solution decays. Thus all initial conditions with Reynolds numbers below this critical value lead to decay.

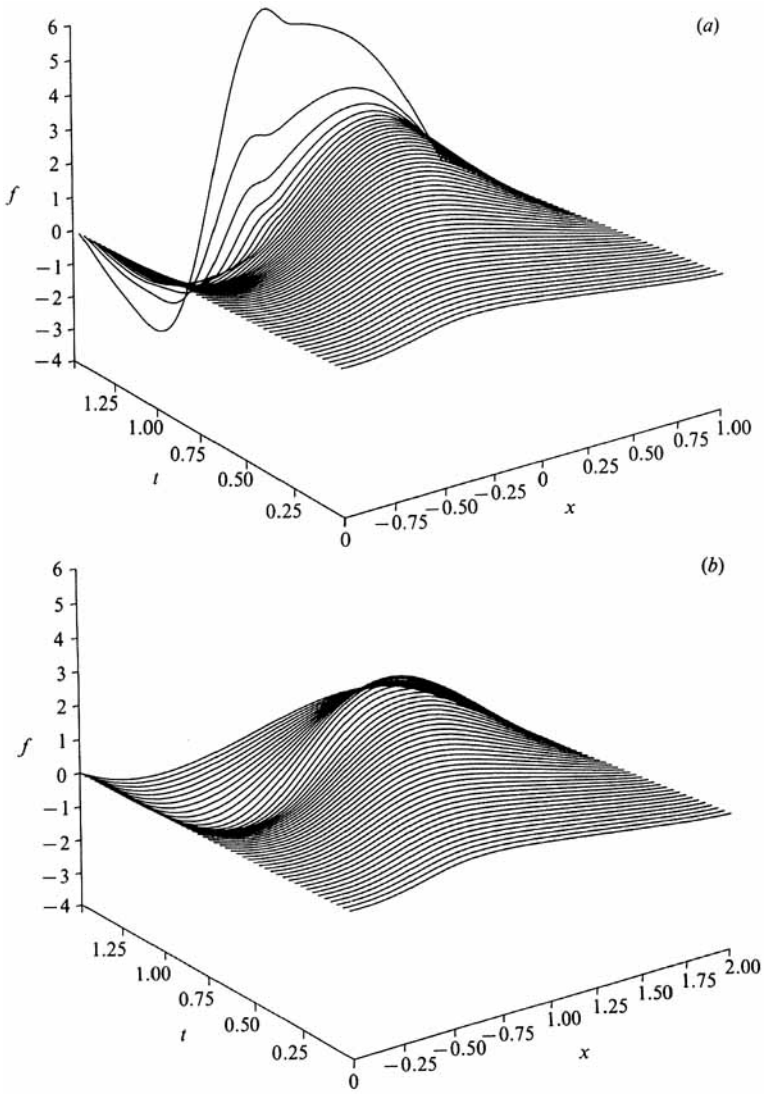


FIGURE 6. Evolution of the profile in figure 5. (*a*) The initial Reynolds number is 6400 and in the last profile, at $t = 1.46$, the Reynolds number has increased to 106541. (*b*) A 250-kink integration of the initial condition in figure 5. Until about $t = 1.24$ there is close agreement with the results in (*a*) but after this the two solutions differ. In fact the kink solution does not track the blow-up of the viscous solution in (*a*).

In (4.4*b*), $\gamma$ is a dimensionless number that we calculate below. Combining these inequalities with (4.1*a*), we have, if $N^{\frac{1}{2}} < 2\nu\gamma/3L^{\frac{3}{2}}$,

$$\dot{N} \leqslant [3\gamma^{-1}L^{\frac{3}{2}}N^{\frac{1}{2}} - 2\nu](4\pi^2/L^2)N. \tag{4.5}$$

If $N^{\frac{1}{2}}$ is initially less than $2\nu\gamma/3L^{\frac{3}{2}}$, then the term in square brackets on the right-hand side is initially negative and becomes more negative as $N$ decreases. It follows that all initial conditions that have $R_0 \equiv N_0^{\frac{1}{2}}L^{\frac{3}{2}}/\nu < 2\gamma/3$ decay. In Appendix A we find $\gamma = 24.3188$ so that the critical Reynolds number is 16.212, i.e. all initial conditions with $R_0$ less than 16.212 ultimately decay. The variational calculation in Appendix A also provides the 'most unstable' initial condition shown in figure 5. Amongst all

initial conditions which satisfy the constraints in (4.3) and have the same initial Reynolds number, $R_0 = N_0^{\frac{1}{2}} L^{\frac{3}{2}}/\nu$, this particular profile maximizes the energy source, $S$, relative to the sink $D$. This profile is therefore an appropriate initial condition for examining singular solutions of the Navier–Stokes equation (1.2$a$).

### 4.2. *Blow-up in finite time of a viscous solution*

Equation (1.2$a$) was solved with the Chebyshev tau method (Gottlieb & Orszag 1977) using as many as 55 polynomials. Nonlinear terms were computed spectrally, without aliasing error. Time stepping was performed with a leap-frog predictor and standard trapezoidal corrector. A typical time step was 0.0002 for the work reported here. Accuracy of evolution was monitored by computing both sides of (4.1$a$) every 250 steps. The relative error was typically 0.005. The Reynolds number of the initial condition was varied between 10 and 6400. Blow-up was considered to have occurred on machine overflow. Solutions remained accurate to an evolved Reynolds number, $R(t) \equiv N(t)^{\frac{1}{2}} L^{\frac{3}{2}}/\nu$, of at least 300000.

A typical experiment, begun with the profile in figure 5, and with $R_0 = 6400$, is shown in figure 6($a$). The last profile displayed is at $t = 1.46$ and has $R = 106541$. Now shown is the subsequent evolution, which produces machine overflow for $t \approx 1.50$. At $t = 1.49$, $R = 297580$. In figure 7($a$) we show $1/R(t)$ versus $t$. Note the changeover from an initial exponential phase of decay of $1/R$, suggesting singularity formation in infinite time, to a sudden break at about $t = 1.4$. In figure 7($b$) we show an expanded view of the knee of the curve. This suggests that the curve cuts the horizontal axis at $t$ slightly greater than 1.49.

We also evolved the same initial condition with $R = \infty$ using from 40 to 250 kinks. The result with 250 kinks is shown in figure 6($b$). Remarkably, there is very close agreement up to approximately $t = 1.25$ (even with as few as 40 kinks), but the kink solution shows no tendency to track the explosive growth of the viscous solution for $t > 1.25$. This is in sharp contrast to the results of §3, where increasing the number of kinks gives results that smoothly tend to the continuous result in (2.17), e.g. figure 3. This divergence between accurate calculation of the partial differential equation and the evolution observed in the inviscid kink approximation suggests that viscous blow-up differs fundamentally from the first example of inviscid singularity formation discussed in §2, i.e. (2.17) *et seq.* In any case it is apparent from figure 6($a$) that concentrated vorticity in a boundary layer is not necessarily associated with the viscous blow-up.

To test the hypothesis that viscous blow-up differs from inviscid, we took (2.17) at $\tau = 2$ (corresponding to $t = 1.4033$) as an initial condition for the viscous problem with $R = 6400$. (Of course this initial condition fails to satisfy boundary conditions on the derivative of $f$, but adjustment takes place after a single time step.) Blow-up occurred after an interval of about 0.65, corresponding to an evolved time of $t = 2.083$, greater than the inviscid result of $t^* = \pi^2/6 \approx 1.645$. This calculation is summarized in figure 8. At first, as the inviscid solution, (2.17), suggests, the gradient of $f$ intensifies on the left-hand side of the domain and one might think that a boundary layer is forming there. However as blow-up is approached, $f$ instead develops a sign change and the vorticity, $-yf_{xx}$, is no longer confined to an increasingly thin layer near $x = 0$. This is in contrast to the inviscid solution in figure 1 and supports our earlier contention, based on figure 6($a$), that viscous blow-up differs fundamentally from the inviscid boundary-layer mechanism. Instead we now argue that the inviscid separable solutions in §2.5 are a closer approximation to the viscous problem.

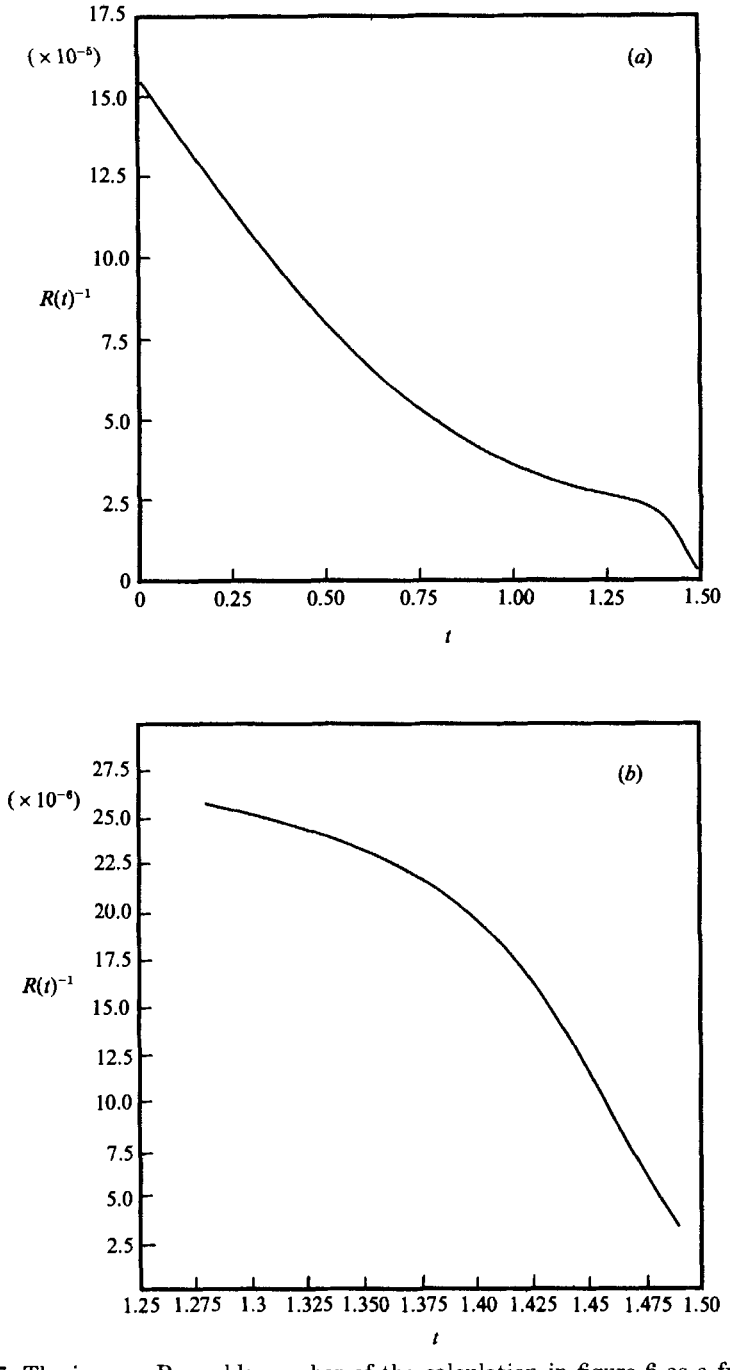


FIGURE 7. The inverse Reynolds number of the calculation in figure 6 as a function of time. (*a*) Evolution over the complete time interval showing an initial gradual decline followed by a sudden break at $t = 1.4$. (*b*) An expanded view of the 'knee' in (*a*). Linear extrapolation suggests blow-up occurs at $t \approx 1.49$.

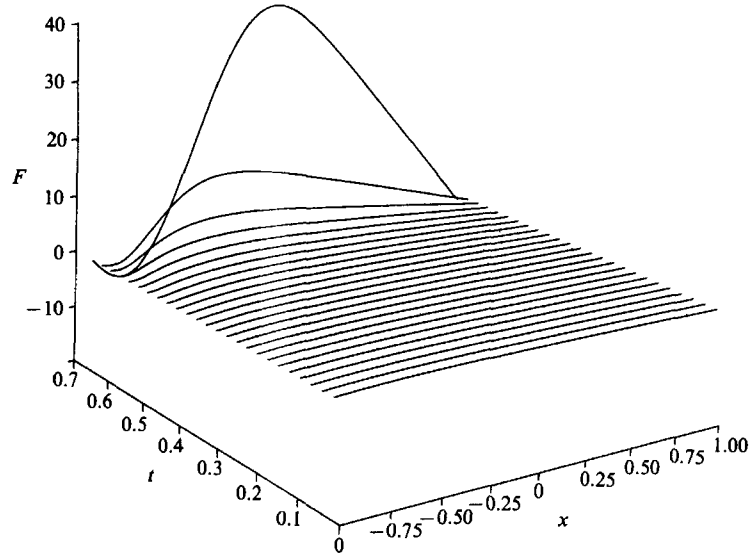


FIGURE 8. Viscous evolution from (2.17) at $\tau = 2$ or $t = 1.4033$. Blow-up occurs after an interval of 0.65. The sign change which develops near $x = 0$ in the last profile is evidence that blow-up is not accompanied by boundary-layer formation.

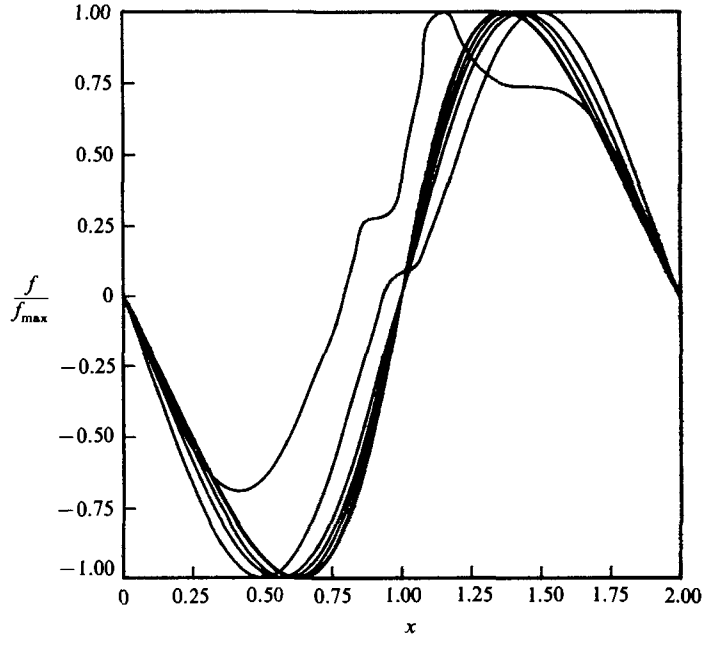


FIGURE 9. Viscous evolution corresponding to figure 2. In order to see if the separability is preserved, all profiles are normalized by $f_{\max}$. Blow−up occurs at $t = 1.3$ and there are ten profiles plotted at equally spaced time intervals of 0.13. The first five profiles coincide to within a line width.

Figure 9 shows the results of viscously evolving the profile in figure 2 starting with a Reynolds number of 6400 and $N_0 = 1$. (Once again, because the inviscid solution does not satisfy the gradient boundary condition there is an initial adjustment which takes a single time step.) Blow-up occurs at $t^* = 1.3$ whereas with $q = 1$ and $L = 2$

the inviscid result in (2.27) is $t^* = 1$. In figure 9, each profile has been normalized by its maximum value so that if the separable structure in (2.26$a$) were preserved, all ten profiles would coincide. But only the first five coincide to within a line width. The last two depart considerably but reveal no tendency to form a boundary layer as blow-up occurs. Instead, in the final stages of blow-up, the profile becomes increasingly disordered, possibly as a result of instabilities on the separable solution that reach finite amplitude.†

We were initially surprised by the failure of the viscous solution to form sharp boundary layers – especially because we thought it should be possible to append passive viscous layers to (2.17) in order to satisfy the gradient condition at $x = 0$ and $x = L$. Thus it is tempting, but incorrect, to suppose that one can match the solution (2.17) with time-dependent boundary layers at $x = 0$ and $L$, chosen to make $f_x$ zero at these endpoints. One reason for the failure of this approach is that, as evaluation of (1.2$a$) at $x = 0$ and $x = L$ shows, when $\nu \neq 0$

$$f_{xxx}(0, t) = f_{xxx}(L, t) = -\nu^{-1}h(t). \tag{4.6}$$

This solution strategy, in which one constructs two boundary layers, each of which communicates only with the interior solution in (2.17), has no way of incorporating (4.6). Indeed, one can show that in the most natural scaling, the two third derivatives are both non-zero and have different orders of magnitude.

## 5. Discussion

We consider first the implications of this study regarding the inviscid case. The surprising feature of the stagnation similitude $(u, v) = (f(x, t), -yf_x(x, t))$, involving a single scalar function $f(x, t)$, is the blow-up in finite time of the functions determining the velocity field and vorticity (here, the function $f$). In the model we have studied, this breakdown is a result of the unboundedness of the initial vorticity, which in turn is a result of the unbounded domain. In this respect the models we have considered here cannot serve as models for three-dimensional singularities of Euler's equations within a bounded domain. As exact solutions, they do tell us something about the capacity of the Euler (and Navier–Stokes) equations to support singular solutions, but the particular form of the singularities, involving velocity fields which blow up *everywhere* in finite time, is very special. Their use is mainly to show that the stagnation-point blow-up which occurs in three dimensions also occurs in two.

In a two-dimensional flow within a bounded domain, the stream function would, when expanded locally in $y$, possess an infinite Taylor series in $y$, with coefficients which couple together in the vorticity equation (1.1). Thus the expansion cannot be closed with the term proportional to $y$, and the singularities obtained with stagnation-point structure do not occur. Blow-up of a single coefficient of an infinite Taylor series representing a function whose singularity will appear on a small set, e.g. a point, is of course to be expected.

The generalization to three dimensions of the stagnation-point similitude is a possible way to obtain exact solutions that model the local behaviour of Euler flows in bounded domains. Such a formulation retains the non-trivial structure in the

† Subtracting the normalized initial condition from the succeeding nine curves in figure 9 gives a smooth antisymmetric residual of fixed form. We anticipate that this represents an eigenmode which could be found from a linear stability analysis of the base profile. We have not verified this, however.

vorticity while effectively localizing it to one space dimension. In this respect, the similitude improves on such non-local singular solutions as

$$(u, v, w) = (t^*-t)^{-1}(y+z, z+x, x+y).$$

As Lin (1958) has shown, Navier–Stokes solutions of the form

$$(u, v, w) = (f_1(x,t), yf_2(x,t)+zf_3(x,t)+f_4(x,t), yf_5(x,t)+zf_6(x,t)+f_7(x,t)) \quad (5.1)$$

are acceptable forms of the stagnation-point similitude. The examples studied by Stuart (1987) are equivalent to taking

$$f_3 = f_4 = f_5 = f_7 = 0, \quad f_1(0,t) = 0, \quad f_2(\infty,t) = 0, \quad f_6(\infty,t) = 1, \quad (5.2)$$

with $L = \infty$. The results of the present paper show that blow-up of such solutions is not a special feature of three-dimensional structure, within the class (5.1) of flows having stagnation-point similitude. This fact makes our study quite different from investigation of three-dimensional singularity structure based upon spectral or vortex-type numerical methods.

The two-dimensional, inviscid examples we have given, although not complete, indicate that blow-up occurs under a wide variety of conditions. The interval may be finite or infinite (with exponential decay of the vorticity for large $x$ in the latter case), $f/f_{\max}$ may or may not depend on time, and $f$ may or may not vanish at an internal point. A precise classification of singularity structure for the inviscid problem, which might be accessible from the Lagrangian representation of solutions, would be of considerable interest in establishing the scope of this non-physical blow-up. Moreover, it would be natural to seek fields which are somewhat less constrained than the flows of stagnation-point form. Analogous forms involving two-dimensional structure would be extremely difficult to analyse, since they would contain classical two-dimensional hydrodynamics as a special case.

The methods of this paper can be applied to other physical problems. For example, if the Boussinesq approximation is made in Euler's equations for an incompressible stratified fluid, the governing equations are

$$\omega_t + u\omega_x + v\omega_y + \phi_x = \nu\nabla^2\omega, \quad \phi_t + u\phi_x + v\phi_y = 0, \quad \phi = \delta\rho/\rho_0. \quad (5.3)$$

The substitution $(u, v, \phi) = (f(x,t), -yf_x(x,t), yg(x,t))$ now leads to a system in $f$ and $g$ which can, in the inviscid case, be studied using the first method of §2. We summarize these results in Appendix B and note that in the case of (5.3) there are apparently no global regularity results paralleling those of Hölder (1933), Wolibner (1933) and Kato (1967) for two-dimensional homogeneous Euler flows. Thus it is not known if solutions of the initial-value problem for the inviscid form of (5.3) in a bounded domain remain regular for all time.

Regarding the viscous case, only a few examples have been considered in this paper, but they clearly indicate that conventional boundary-layer reasoning is inadequate for dealing with the dynamic growth which occurs at the singularity. The understanding of the viscous evolution probably requires analysis of the reduced equation which renormalizes the blow-up. Setting

$$f(x,t) = (t^*-t)^{-1}F(x,\tau), \quad \tau = -\ln(t-t), (t^*-t)^2h(t) = h^*(\tau),$$

we see that (1.2$a$) gives

$$F_{x\tau} + F_x + FF_{xx} - F_x^2 - \nu e^{-\tau}F_{xxx} = h^*(\tau). \quad (5.4)$$

We can therefore regard the viscous correction as a global forcing term which is exponentially small at large $\tau$. If we take an inviscid solution from the class discussed in §2.5, then $F$ would be a steady solution of the inviscid form of (5.4). If, however, this solution were unstable on the timescale $\tau$, then the viscous forcing in (5.4) could produce an $O(1)$ change in $F(x,\tau)$. This may be the process we are seeing in the viscous calculations at the phase of explosive blow-up, although such an explanation is tentative. It is also possible that ultimately the singularity is arrested by fine structure created during the explosive phase. In any event the analysis of this phase of the blow-up is the most interesting problem for future work suggested by the present study.

We thank M. R. E. Proctor for a helpful discussion. A part of this work was done at the 1987 Woods Hole Summer Study Program in Geophysical Fluid Dynamics. We thank the director of the 1987 Program, Willem V. R. Malkus, for an enjoyable and stimulating program. G. R. I. and W. R. Y. were supported by the Office of Naval Research under N00014-86-K-0325. S. C. was supported by the National Science Foundation under Contract DMS-831-2229 and by the National Aeronautics and Space Administration under Contract NASA-NAGU-781, at the Courant Institute of Mathematical Sciences, New York University. E. A. S. received support from the National Science Foundation under grant NSF-PHY80-27321.

## Appendix A. Calculation of $\gamma$

To calculate $\gamma$ in (4.4$b$) we consider the variational problem of minimizing the functional in (A 1) over the class of functions which satisfy the constraints in (4.3). The first of these can be imposed as a restriction on the admissible functions. The second is incorporated using a Lagrange multiplier. Thus consider the functional

$$\mathscr{F}[g] = D^2N - \alpha S^2 + \beta I, \tag{A 1$a$}$$

$$D \equiv \int_0^L g'^2\,\mathrm{d}x, \quad N \equiv \int_0^L g^2\,\mathrm{d}x, \tag{A 1$b,c$}$$

$$S \equiv \int_0^L g^3\,\mathrm{d}x, \quad I \equiv \int_0^L g\,\mathrm{d}x, \tag{A 1$d,e$}$$

where $\alpha$ and $\beta$ are Lagrange multipliers and $g$ is zero at $x = 0$ and $x = L$; $\beta$ is picked so that $I = 0$ and $\alpha$ so that $S = L$. (In this Appendix it is convenient to regard $g$ as a dimensionless function.)

The Euler–Lagrange equation obtained from the first variation is

$$g'' - \left(\frac{D}{2N}\right)g + \left(\frac{3S}{2DN}\right)\alpha g^2 - \left(\frac{\beta}{4DN}\right) = 0. \tag{A 2}$$

If this equation is multiplied by $g$ and integrated from $x = 0$ to $x = L$ one finds

$$\alpha = \frac{D^2N}{S^2}. \tag{A 3}$$

Next, if (A 2) is integrated from $x = 0$ to $x = L$ one has

$$[g']_0^L + \frac{3DN}{2S} - \frac{L\beta}{4DN} = 0, \tag{A 4}$$

and it is easy to see from the results below (specifically A 7) that $g'(0) = g'(L)$ so finally

$$\beta = \frac{6D^2N^2}{SL}. \tag{A 5}$$

Together (A 3) and (A 5) remove the unknown multipliers from (A 2) and to summarize

$$g'' - \left(\frac{D}{2N}\right)g + \left(\frac{3D}{2S}\right)\left[g^2 - \left(\frac{N}{L}\right)\right] = 0. \tag{A 6}$$

A first integral is obtained in the usual way:

$$g'^2 + V(g) = \left(\frac{3D}{2L}\right), \quad V(g) = -\left(\frac{D}{2N}\right)g^2 + \left(\frac{3D}{S}\right)\left[\tfrac{1}{3}g^3 - \left(\frac{N}{L}\right)g\right], \tag{A 7$a,b$}$$

and the constant of integration on the right-hand side of (A 7$a$) follows from the integral over the interval $(0, L)$.

Equation (A 6), or equivalently (A 7), is the Euler–Lagrange equation. If $g$ is a solution of this nonlinear problem then so is $kg$ where $k$ is any constant. Thus, although we used the normalization $S = L$ in formulating the variational problem, alternatives, such as $N = L$, are obtained by rescaling $g$. Also, because $D^2N/S^2$ is independent of $k$, the minimum value of this homogeneous quotient over all functions which satisfy (4.3) is given by the solution of (A 6). A numerical technique, described below, produces

$$N = 1.2276L, \quad D = 21.9486L^{-1} \tag{A 8}$$

and the extremizing function $g$, together with $f = \int_0^x g\,\mathrm{d}x$, is plotted in figure 5. These numerical results give

$$\min_g \frac{D^2N}{S^2} = 591.40L^{-3} \tag{A 9}$$

or in (4.4$b$), $\gamma = 24.318$.

To solve (A 6) numerically one represents $g(x)$ as

$$g(x) = \sum_{n=1}^{N} g_n T_n\left(\frac{2x-L}{L}\right), \tag{A 10}$$

where $T_n(z)$ is the $n$th Chebyshev polynomial. Boundary conditions are enforced in the usual manner by the tau method. Equation (A 6) is viewed as an $N-2$ component vector-valued functional, $\mathscr{K}(g)$. We look for a zero of $\mathscr{K}$ with Newton's method. Convergence is rapid for $N \geqslant 30$, from even a poor initial guess, with no evidence of multiple solutions.

## Appendix B. An inviscid sedimentation problem

We summarise results for the solution of (5.3) with $\nu = 0$. The substitution introduced following (5.3) yields the system

$$\mathrm{L}[f_x] = g(x_0, t) + h(t), \quad \mathrm{L}[g] = 0. \tag{B 1}$$

We shall apply the first method of §2 to (B 1). Proceeding as in §2.1, see that $g = g_0(x_0)\,J, f_x = -\dot{\phi}J$, where

$$\ddot{\phi}_1 + h(t)\,\phi_1 + g_0(x_0) = 0, \quad \phi_1(0) = 1, \quad \dot{\phi}_1 = 0. \tag{B 2}$$

These initial conditions ensure that the initial velocity is zero.

We may solve (B 2) by setting $\phi = \phi_1(t) + g(x_0)\,\phi_2(t)$ where

$$\ddot{\phi}_1 + h(t)\,\phi_1 = 0, \quad \phi_1(0) = 1, \quad \dot{\phi}_1 = 0, \tag{B 3a}$$

$$\ddot{\phi}_2 + h(t)\,\phi_2 + 1 = 0, \quad \phi_2(0) = \dot{\phi}_2 = 0. \tag{B 3b}$$

The condition that determines $h(t)$ is, as in §2, the condition on the Jacobian,

$$L^{-1}\int_0^L (\phi_1 + g(x_0)\,\phi_2)^{-1}\,\mathrm{d}x_0 = 1. \tag{B 4}$$

As an example, we take $g_0 = \mathrm{e}^{-\lambda x_0}$, $\lambda > 0$. Then (B 4) yields

$$\phi_2 = G(\phi_1) \equiv \frac{\phi_1 k^{\phi_1} - k\phi_1}{1 - k^{\phi_1}}, \tag{B 5}$$

where $k = \mathrm{e}^{\lambda L}$. If (B 5) is used to eliminate $h(t)$ from (B 3), the equation for $\phi_1$ may be integrated once and then expressed as an integral over $\phi_1$. The time to blow-up is then given, for $\lambda L = 2$, by

$$t^* = \sqrt{2}\int_1^\infty \mathrm{d}\phi\phi^{-2}\left[\int_1^\phi \phi(G - \phi G')\,\mathrm{d}\phi\right]^{\frac{1}{2}} \approx 2.0012. \tag{B 6}$$

It is again easy to implement a 'kink' model utilizing a piecewise linear representation for $f$ and a piecewise constant function in place of $g$. Without giving details we simply note that for the above example the blow-up does not occur in a finite kink model, just as in the Euler flow problem. With $\lambda L = 2$, the maximum amplitude of $f$ is found to occur at time 2.136 with 25 kinks, at time 2.0855 with 50 kinks, and at time 2.0530 with 100.

## REFERENCES


Aref, H. 1983 Integrable, chaotic, and turbulent vortex motion in two-dimensional flows. *Ann. Rev. Fluid Mech.* **15**, 345–389.

Batchelor, G. K. 1967 *An Introduction to Fluid Dynamics*. Cambridge University Press.

Drazin, P. G. 1983 *Solitons*. Lond. Math. Soc. Lecture Notes Series, vol. 85. Cambridge University Press.

Gottlieb, D. & Orszag, S. A. 1977 *Numerical Analysis of Spectral Methods. Theory and Applications*. CBMS Regional Conference Series in Applied Mathematics, vol. 26, Society for Industrial and Applied Mathematics, Philadelphia.

Hölder, E. 1933 Über die un beschränkte Fortsetzbarkeit einer stetigen abenen Bewegung in einer unbegretzen inkompressiblen Flüssigkeit. *Math. Z.* **37**, 727–738.

Howarth, X. X. 1951 The boundary layer in three-dimensional flow. Part 2. The flow near a stagnation point. *Phil. Mag.* **42**, 1433–1440.

Kato, T. 1967 On the classical solution of the two-dimensional, non-stationary Euler equation. *Arch. Rat. Mech. Anal.* **25**, 188–200.

Lin, C. C. 1958 Note on a class of exact solutions in magnetohydrodynamics. *Arch. Rat. Mech. Anal.* **1**, 391–395.

Stuart, J. T. 1987 Nonlinear Euler partial differential equations: singularities in their solution. In *Symposium to Honor C. C. Lin* (ed. D. J. Benney, F. H. Shu & C. Yuan). World Scientific.

Wolibner, W. 1933 Un theorème sur l'existence du mouvement plan d'un fluide parfait, homogène, incompressible, pendent un temps infiniment long. *Math. Z.* **37**, 698–726.